Alignment of Gaussian beams

W. B. Joyce and B. C. DeLoach

The design of a coupling between a semiconductor laser and a single-mode fiber, or between any two optical or acoustical elements that support Gaussian modes, is presented as a trade-off among coupling efficiency T_a, offset misalignment tolerance d_e, and angular misalignment tolerance θ_e. We show that these three parameters are subject to a trade-off limitation which takes the form $0 < T_a^{1/2}\theta_e d_e \leqslant \lambda/\pi$, and we show how to design a coupling so that the upper bound on the alignment product $T_a^{1/2}\theta_e d_e$ is achieved.

I. Introduction

The efficiency of optical-power transmission from a single-mode semiconductor laser into a single-mode fiber, or through an optical-fiber splice, or between other pairs of optical or acoustical elements is often reduced by the practical limitations of either the initial alignment accuracy or the long-term alignment stability. As a consequence we analyze in this work the coupling efficiency between two Gaussian beams. Our guiding theme is not, however, the maximization of coupling efficiency *per se*; rather we develop implications of the fact that coupling efficiency can be traded away to achieve more relaxed alignment tolerances.

In Sec. II some useful properties of Gaussian beams are summarized. In Sec. III the coupling efficiency between two aligned (coaxial) beams is determined. Then in Secs. IV and V the tolerances for misalignment are evaluated. In Sec. VI it is shown that the coupling efficiency and the alignment tolerances can, with appropriate design changes, be separately increased up to a certain bound. Beyond this bound, however, a trade-off limitation sets in. This limitation implies that any design change which yields a further increase in any one of three quantities (coupling efficiency, angular misalignment tolerance, offset misalignment tolerance) necessarily decreases at least one of the other two. Section VII presents a procedure for designing a coupling with any prescribed values of coupling efficiency and misalignment tolerance that are permitted by the previously derived bound. As an example, a brief application to laser–fiber coupling is given in Sec. VIII.

The authors are with AT&T Bell Laboratories, Murray Hill, New Jersey 07974.

Received 23 July 1974.
0003-6935/84/234187-10$02.00/0.

II. Gaussian Beams

Figure 1 shows a Gaussian beam (= Gaussian mode) as it focuses down to its waist ($2w_0$ at $z = 0$) and then diverges to the right. At a z plane (plane perpendicular to the z axis at z) the width has increased to $2w$; that is, the amplitude is down by $1/e$ at $x = w$, and the intensity is down by $1/e$ at $x = 2^{-1/2}w$. Also, at the z plane, a surface of constant phase has radius R and curvature $\kappa = 1/R$. Under various circumstances it is useful to characterize the beam at z by different pairs of these parameters (z, w_0, w, and κ or combinations thereof): In the local representation, the beam is described by its size (halfwidth) w and curvature κ at the z plane of interest. Alternately, in the waist-spacing representation the beam is described by its waist size w_0 and the distance z of the z plane of interest from the waist. If w_0 and z are known, κ and w at z are found from[1,2]

$$R = 1/\kappa = z[1 + (kw_0^2/2z)^2] \tag{1}$$

and

$$w = w_0[1 + (2z/kw_0^2)^2]^{1/2}, \tag{2}$$

where $k = 2\pi/\lambda$ and $-\infty < z < \infty$. Equation (1) shows that negative z yields negative κ and R; i.e., a surface of negative radius is convex as seen from the left. Alternatively, if w and κ are known, elimination of z from Eqs. (1) and (2) yields the waist size w_0,

$$1/w_0^2 = 1/w^2 + (\tfrac{1}{2}kw\kappa)^2, \tag{3}$$

and Eq. (2) is then trivially solved for the corresponding z. Note that w and κ are unrestricted independent variables; that is, from Eq. (3), and then Eq. (2), it is apparent that there is a pair of values w_0 and z (with $0 < w_0 \leqslant w$) corresponding to any pair of values for w and κ. (In this work any values or every case refers to the physical range $0 < w < \infty$ and $-\infty < \kappa < \infty$.)

Because of aperturing and other effects, beams of interest are typically only approximately Gaussian. Thus the practical application of Gaussian theory often requires that a beam be represented by its most nearly

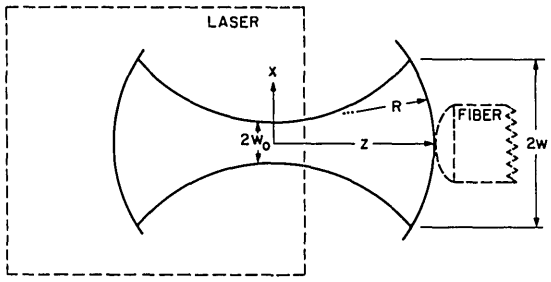

Fig. 1. Parametrization of a Gaussian beam.

equivalent Gaussian mode. For crude purposes a two-point fit at the $1/e$ intensity points or at the half-power points may suffice. A better choice is usually that Gaussian which has the maximum projection on (inner product with) the actual beam. Marcuse has developed this projection procedure for optical fibers, and he gives explicit prescriptions for a variety of index profiles.[3] For example, for a fiber consisting of a uniform core of radius a and index n_1 in an infinite cladding of index n_2, he finds empirically that the size w of the Gaussian approximation to the fiber mode is given by

$$w = a(0.65 + 1.619V^{-3/2} + 2.879V^{-6}) \quad (4)$$

for $V \gtrsim 1.2$, where V is defined by

$$V^2 = (n_1^2 - n_2^2)k^2a^2, \quad (5)$$

and k has its free-space value.

If, for example, the vertical dashed lines in Fig. 1 are interpreted as the mirrors of a gain-guided laser, the waist of the beam emitted from the laser is a virtual waist inside the laser.[4] In a typical experimental procedure the intensity profile at the virtual waist is inferred from a near-field scan with focusing at the z plane of minimum spot size. Then w_0 is chosen to fit this scan while the waist position (origin for z) is placed inside the laser by the distance a remotely focused lens moves when it first images the mirror face (externally illuminated by light of the emission wavelength) and then images the plane of minimum spot size. Alternately w_0 and the z origin are chosen so that the scan of a given plane (e.g., the mirror) transforms best (maximum projection) into the observed far-field pattern.

Figure 1 illustrates a common, and certainly valid, representation of the coupling problem: A mode is emitted from the source (e.g., a laser). The mode then expands as it crosses the gap, if any. Finally, the wave front of the mode falls on the sink (e.g., a fiber) where it is recurved by the lens and then projected onto the fiber mode to determine the coupling efficiency. However, in the present work we use an alternative conceptualization that decouples certain elements of the design problem and typically leads to different thought patterns: In Fig. 2 a Gaussian mode leaves the source (as in Fig. 1). In addition the mode of the sink is extended back into the gap. (Think of light propagating backward in the fiber of Fig. 2.) Details of the source and sink can then be forgotten; each is completely represented by the size and position of its waist. The waist associated with one element (source or sink) may be a real waist in the gap (Fig. 2), a virtual waist inside the element (Fig. 1), or a virtual waist inside the other element. The first step of the design problem, as treated in the remainder of this work, consists of choosing the sizes ($\bar{w}_0$ and w_0) and locations of the two waists to yield the desired coupling efficiency and alignment tolerances.

The second step of the design problem, which we do not consider here, is as much an art as a science. It consists, for each element, of choosing among the innumerable possible combinations of lenses, inhomogeneous absorption, converging[5–7] or diverging tapers, or other[8] transformers a particular more readily manufactured combination which yields, to the extent practical, a waist of the desired size, position, and freedom from aberration. (For an analysis of aberration in the laser–fiber context see Ref. 9. To realize the potential accuracy of an aberration calculation, it is often necessary to go beyond the Gaussian model when describing the beam of a given laser. The actual laser

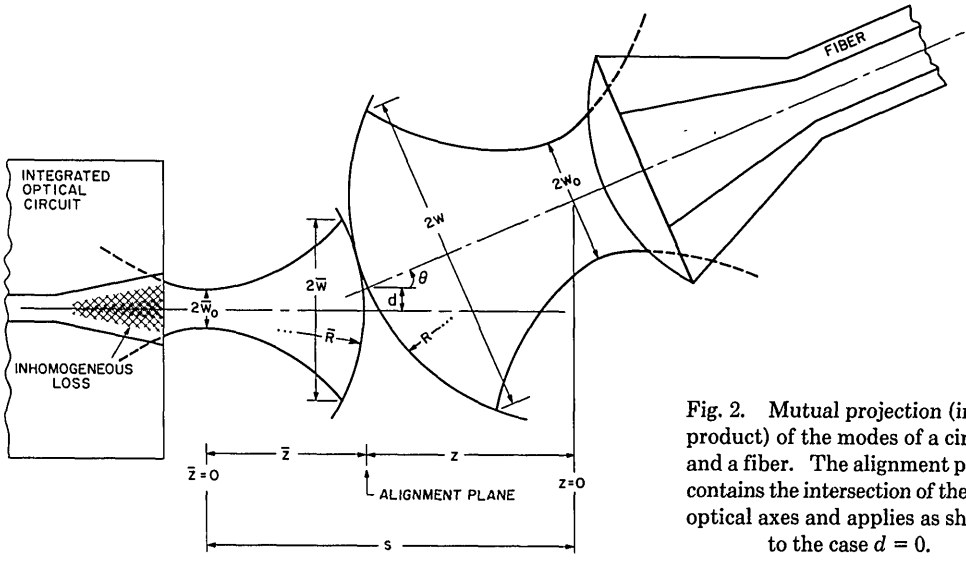

Fig. 2. Mutual projection (inner product) of the modes of a circuit and a fiber. The alignment plane contains the intersection of the two optical axes and applies as shown to the case $d = 0$.

beam can be usefully represented as a fundamental Gaussian plus higher-order Hermite-Gaussian modes[1] or, approximately, as a Gaussian distorted by standard aberrations. The latter representation suggests directly the desired compensating aberrations of the optics.)

III. Aligned Coupling Efficiency

This section reproduces, with slight modifications to admit ellipticity, Kogelnik's evaluation of the coupling efficiency between two aligned (coaxial) Gaussian beams.[1]

Laser beams are often elliptical because, for example, of differences in the degree of mode confinement in the x and y directions or because of astigmatism; e.g., the gain-guided waist in the x-z plane is displaced by some Δz from the real-index-guided waist at the mirror in the y-z plane (Fig. 1.) We consider the simple case where either the x and y beam axes of the source and sink are rotationally (around the z axis) aligned with negligible error or else one of the elements (e.g., the fiber) has rotational symmetry (circular mode). Then the x and y coordinates are chosen to fall along the major and minor axes of the elliptical field of the other element (e.g., the source). In this coordinate system a Gaussian beam of amplitude Ψ factors, i.e., at a particular z plane,

$$\Psi(x,y) = \psi(x,w_x,\kappa_x)\psi(y,w_y,\kappa_y), \tag{6}$$

and the x-z plane and y-z plane alignments can be analyzed virtually independently of each other. (Because the source–sink spacing is necessarily the same for both analyses and because circular rather than cylindrical lenses may be dictated, the analysis in one plane may involve constraints imposed by the solution in the other plane.[10])

At the projection plane, i.e., the z plane where the source mode is projected onto the sink mode, the normalized sink field ψ or $|>$ is, with perfect alignment ($d = \theta = 0$ in Fig. 2)

$$|w,\kappa> = \psi(w,\kappa;x) = (2/\pi)^{1/4}w^{-1/2}\exp[-(x/w)^2 + \tfrac{1}{2}ik\kappa x^2]. \tag{7}$$

The x-z plane power transmissivity or coupling efficiency τ_a for the aligned case is the squared absolute value of the inner product,[1,11,12]

$$\tau_a = |\langle\overline{w},\overline{\kappa}|w,\kappa\rangle|^2 = \left|\int_{-\infty}^{\infty}\psi^*(\overline{w},\overline{\kappa};x)\psi(w,\kappa;x)dx\right|^2 \tag{8}$$

$$= \frac{2}{[(\overline{w}/w + w/\overline{w})^2 + (\tfrac{1}{2}k\overline{w}w)^2(\overline{\kappa}-\kappa)^2]^{1/2}}. \tag{9}$$

Equation (9) expresses τ_a in the local representation, i.e., in terms of the beam sizes ($\overline{w}$ and w) and curvatures ($\overline{\kappa}$ and κ) at the projection plane. In terms of the waist sizes ($\overline{w}_0$ and w_0) and the distances ($\overline{z}$ and z) from the waists to the projection plane, Eq. (9) becomes[1] with the aid of Eqs. (1)–(3)

$$\tau_a = \frac{2}{[(\overline{w}_0/w_0 + w_0/\overline{w}_0)^2 + (2/k\overline{w}_0w_0)^2s^2]^{1/2}}. \tag{10}$$

As expected from physical considerations, τ_a depends on the separation $s = \overline{z} - z$ between the waists but not on the position $\overline{z}$ or z of the projection plane. For optical, rather than mechanical, purposes, it is convenient to define the distance between the source and the sink as the waist separation s.

From Eq. (10) it is apparent that, as source and sink are brought together, $\tau_a(s)$ passes through a maximum $\tau_a(0) = \tau_a(s = 0)$ when the waists cross where

$$\tau_a(s) \leqslant \tau_a(0) = \frac{2}{\overline{w}_0/w_0 + w_0/\overline{w}_0}. \tag{11}$$

(When neither waist is outside its element, as with a gain-guided laser and an unlensed fiber, it may, of course, be mechanically impossible to reach the crossing point.)

We interpret Eq. (9) or (10) as the x-z plane transmissivity $\tau_{a,x}$. In the y-z plane the same expressions yield $\tau_{a,y}$ if the y-z plane beam parameters are used. From Eqs. (6) and (8) the aligned power transmissivity T_a from the source into the sink is

$$T_a = \tau_{a,x}\tau_{a,y}, \tag{12}$$

which is equivalently written as

$$-10\log T_a = -10\log\tau_{a,x} - 10\log\tau_{a,y}. \tag{13}$$

Equation (13) states that the total number of decibels of aligned coupling loss is simply the sum of the number of decibels assigned to the x-z and y-z planes. For a circular beam Eq. (12) reduces to

$$T_a = \tau_a^2. \tag{14}$$

Thus for a circular beam τ_a can be replaced in the remainder of this paper by $T_a^{1/2}$.

IV. Tilt and Offset Tolerances

The mode (barred variables) emitted from the source in Fig. 2 is imperfectly injected into the mode (unbarred variables) of the sink not only because of a mismatch of mode size ($\overline{w} \neq w$) and curvature ($\overline{\kappa} \neq \kappa$) but also because of any unintentional offset d or tilt angle θ between the modes. Thus when developing a coupling package one may have to design in adequately large tolerances for offset and tilt misalignment. The need for these tolerances is dictated by initial alignment limitations (e.g., micromanipulator limitations) and also by subsequent effects such as thermal-expansion misalignment and long-term (decades in an undersea optical cable) creep of any relevant solders or resins etc. Alternatively, for example, in a self-aligning package based on crystallographic planes plus cleaving and etching, a laser's stripe and optical axis may be imperfectly oriented with respect to its mirror plane, either initially or because of beam wander with aging. At the other extreme an optical coupling may serve as a transducer which measures displacement or angle, and low misalignment tolerance (high sensitivity) may be desired for one (and only one) observable. Motivated by such applications we now turn to the quantification of the alignment tolerance.

To analyze tilt misalignment it is necessary to choose an alignment plane, i.e., a z plane defined by the point on the z axis about which the rotation angle θ occurs. (Typically more than one alignment plane is of interest, as determined, for example, by micromanipulator error or by the z position of the y axis of vibrational or rota-

tional strain of each element with respect to its mounting.) For convenience we will take the projection plane at the alignment plane. Thus when the alignment plane is in the gap (Fig. 2 with $d = 0$) the projection involves real modes. When the alignment plane intersects an optical element, the projection involves the virtual continuations of the real modes of the gap (dashed arcs in Fig. 2).

Tilt of the sink through θ introduces, in the small-angle approximation, the additional phase angle $k\theta x$ into the exponent of Eq. (7), i.e., in the alignment plane[1]

$$|w,\kappa;\theta> = (2/\pi)^{1/4} w^{-1/2} \exp\{-(x/w)^2 + i[k\theta x + \tfrac{1}{2}k\kappa x^2]\}. \quad (15)$$

Thus in the presence of tilt the transmissivity becomes[12]

$$\begin{aligned} \tau &= |\langle \overline{w},\overline{\kappa},0|w,\kappa,\theta\rangle|^2 \\ &= \tau_a \exp[-(\theta/\theta_e)^2], \end{aligned} \quad (16)$$

where τ falls off by $1/e$ in an angle θ_e given, in the local (alignment-plane) representation, by

$$\theta_e = \frac{2^{3/2}}{k\tau_a(\overline{w}^2 + w^2)^{1/2}} = \frac{2^{1/2}}{\pi\tau_a[(\overline{w}/\lambda)^2 + (w/\lambda)^2]^{1/2}} \quad (17)$$

with $\tau_a = \tau_{a,x}$ from Eq. (9). The alternative representation for the angular tolerance θ_e in terms of the waist sizes ($\overline{w}_0$ and w_0) and their distances ($\overline{z}$ and z) to the alignment plane can be written down by inspection from Eqs. (2), (10), and (17). Multiplication of Eq. (16) by $\tau_{a,y}$ yields

$$T = T_a \exp[-(\theta/\theta_e)^2]. \quad (18)$$

Equation (18) applies to tilt in either plane if $\overline{w}$ and w in Eq. (17) are the halfwidths in the plane of the tilt. Further properties of θ_e are given in Eqs. (42) and (50).

Offset (x-direction displacement d with the axes of the two modes remaining parallel) is indistinguishable from an infinitesimal tilt $\theta = d/z$ about an axis at $z = \infty$. Thus the effect of offset on coupling efficiency must be a special case of Eq. (16). As $z \to \infty$, introduce $\theta = d/z$ as well as $w \to 2z/kw_0$ and $\overline{w} \to 2\overline{z}/k\overline{w}_0$ [from Eq. (2)] into Eqs. (16) and (18). Then for fixed s and large $z = \overline{z} - s$ Eqs. (16) and (18) become

$$\tau = \tau_a \exp[-(d/d_e)^2], \quad (19)$$

$$T = T_a \exp[-(d/d_e)^2], \quad (20)$$

where

$$d_e = \frac{2^{1/2}}{\tau_a(1/\overline{w}_0^2 + 1/w_0^2)^{1/2}}, \quad (21)$$

with τ_a given by Eq. (10) in the waist-spacing representation. As with tilt in Eqs. (16) and (18), it can be seen that Eqs. (19) and (20) apply to offset in either plane provided that τ_a and d_e are evaluated in the same plane. Equations (17), (18), (20), and (21) are, of course, immediately applicable to circular beams. It follows from Eqs. (11) and (21) that $d_e(s)$ has a minimum at $s = 0$ given by

$$d_e(s) \geq d_e(0) = 2^{-1/2}(\overline{w}_0^2 + w_0^2)^{1/2}. \quad (22)$$

Equation (21) states the useful fact that the product $\tau_a d_e$ is conserved as the waist separation s is varied. ($T_a^{1/2} d_e$ is independent of s for a round beam.) Like τ_a, the offset tolerance d_e depends on the waist sizes and their separation but not on the distances to any reference planes. In contrast $\overline{w}^2 + w^2$, and hence θ_e, depends also on the position of the rotation axis. Thus we hereafter understand the alignment plane to be determined by the rotation axis of physical interest [i.e., not by the rotation axis at $z = \infty$, which was invoked only as an artifice to obtain Eqs. (19)–(21)].

For future reference note that in the local (alignment-plane) representation d_e is found by introducing Eq. (3) into (21); i.e.,

$$d_e = \frac{2^{1/2}}{\tau_a[1/\overline{w}^2 + 1/w^2 + (\tfrac{1}{2}k\overline{w}\overline{\kappa})^2 + (\tfrac{1}{2}kw\kappa)^2]^{1/2}}, \quad (23)$$

where τ_a is now given by Eq. (9).

Figure 2 illustrates the simultaneous presence of tilt θ and offset d at the alignment plane. Instead of deriving explicit expressions for this case we simply remark that this is equivalent to tilt alone about the point where source and sink axes intersect. Thus Eq. (16) applies to simultaneous tilt and offset provided that θ is the tilt angle and $\overline{w}$ and w are the sizes of the beams at the point where the axes intersect.

V. Axial Tolerance

As discussed more fully in Secs. VI and VIII, the increase in the offset tolerance d_e that can be achieved by trading away a given amount of coupling efficiency is greater if the waists are made unequal ($\overline{w}_0 \neq w_0, s = 0$) than if the waists are separated ($s \neq 0$). Thus, since excessively small d_e is usually the main alignment limitation in laser–fiber communication systems, it is often desirable to design at $s = 0$. Similarly, design at $s = 0$ also commonly results from the fact [Eq. (11)] that this is the separation which maximizes the coupling efficiency between a given source and sink. Thus we look more closely at the axial-tolerance expression [Eq. (10)] for the case $s = 0$.

Experimentalists often fit their observed axial dependence of aligned coupling efficiency to the Gaussian form

$$\tau_a(s) = \tau_a(0) \exp[-(s/s_e)^2]. \quad (24)$$

Thus we fit Eq. (24) to Eq. (10) by matching at $s = 0$ (i.e., not at $1/e$ or half-power points). Then

$$\begin{aligned} s_e &= (-\tfrac{1}{2}\tau_a^{-1}\partial^2\tau_a/\partial s^2)_{s=0}^{-1/2} \\ &= 2^{1/2} k\overline{w}_0 w_0/\tau_a(0) \\ &= 2^{-1/2} k(\overline{w}_0^2 + w_0^2). \end{aligned} \quad (25)$$

As an alternative to the rather arbitrary Gaussian fit, we simply regard Eq. (25) as a definition of the tolerance to axial separation around $s = 0$. It is often convenient to take the wavelength $\lambda = 2\pi/k$ in the gap as the unit of distance. Thus we also write Eq. (25) as

$$s_e/\lambda = 2^{1/2}\pi[(\overline{w}_0/\lambda)^2 + (w_0/\lambda)^2] \quad (26)$$

to illustrate the dimensionless form that is a natural

alternative for many of our results. For nonastigmatic elliptical beams (x-z plane and y-z plane waists for each element occur at the same z position), Eqs. (12) and (24) yield

$$T_a(s) = T_a(0)\exp[-(s/S_e)^2], \tag{27}$$

where

$$1/S_e^2 = 1/s_{e,x}^2 + 1/s_{e,y}^2, \tag{28}$$

and $s_{e,x}$ and $s_{e,y}$ are given by Eq. (25). [For astigmatic beams the forms of Eqs. (27) and (28) are still valid.[13]]

Comparison of Eqs. (22) and (25) yields

$$s_e/\lambda = 2^{3/2}\pi[d_e(0)/\lambda]^2, \tag{29}$$

or, for nonastigmatic beams, from Eq. (28)

$$8\pi(S_e/\lambda)^{-2} = [d_{e,x}(0)/\lambda]^{-4} + [d_{e,y}(0)/\lambda]^{-4}. \tag{30}$$

For astigmatic beams see Ref. 13. Equation (29) or (30) shows that at $s = 0$ the axial tolerance s_e or S_e cannot be specified independently of the offset tolerance d_e.

VI. Alignment Product

From Eqs. (9), (17), and (23) it is apparent that large transmissivity ($\tau_a = 1$) and arbitrarily large θ_e and d_e can be separately achieved by appropriate choice of $\overline{w}$,$\overline{\kappa}$,w, and κ. The essential issue, however, is the extent to which large τ_a, θ_e, and d_e can be simultaneously achieved. To investigate this we define the alignment product A:

$$A = \tau_a\theta_e d_e \tag{31}$$

(which reduces to

$$A = T_a^{1/2}\theta_e d_e \tag{32}$$

in the case of a round beam) and the normalized alignment product α:

$$\alpha = \tfrac{1}{2}kA = \tfrac{1}{2}k\tau_a\theta_e d_e. \tag{33}$$

From Eqs. (17) and (21)

$$\alpha = \frac{2}{\tau_a(\overline{w}^2 + w^2)^{1/2}(1/\overline{w}_0^2 + 1/w_0^2)^{1/2}} \tag{34}$$

in a mixed representation or, with Eqs. (9) and (23),

$$\alpha^2 = (\tfrac{1}{2}k\tau_a\theta_e d_e)^2 = \frac{(\overline{w}/w + w/\overline{w})^2 + (\tfrac{1}{2}k\overline{w}w)^2(\overline{\kappa} - \kappa)^2}{(\overline{w}/w + w/\overline{w})^2 + (\overline{w}^2 + w^2)[(\tfrac{1}{2}k\overline{w}\overline{\kappa})^2 + (\tfrac{1}{2}kw\kappa)^2]} \tag{35}$$

in the local representation.

As an example consider a fiber splice with negligible air gap ($\overline{w} = w$, $\overline{\kappa} = \kappa = 0$). Then $\tau_a = 1$ [Eq. (9)], $\alpha = 1$ [Eq. (35)], and Eq. (33) becomes

$$\theta_e d_e = 2/k = \lambda/\pi. \tag{36}$$

This trade-off between angle and displacement tolerance for fiber splices was found numerically for exact fiber modes by Cook *et al.*[14] and derived analytically for Gaussian modes by Marcuse.[3]

We turn now to our central question: What is the maximum value of the non-negative product α, and what are all the combinations of the four independent variables $\overline{w}$, $\overline{\kappa}$, w, and κ that achieve this maximum? To answer this multiply out the curvature factors in Eq. (35) and note that α^2 is of the form

$$\alpha^2 = \frac{F + G}{F + H} \tag{37}$$

with

$$F = \left(\frac{\overline{w}}{w} + \frac{w}{\overline{w}}\right)^2 + (\overline{w}w)^2[(\tfrac{1}{2}k\overline{\kappa})^2 + (\tfrac{1}{2}k\kappa)^2] > 0$$

$$G - H = -2(\tfrac{1}{2}k\overline{w}^2\overline{\kappa})(\tfrac{1}{2}kw^2\kappa) - (\tfrac{1}{2}k\overline{w}^2\overline{\kappa})^2 - (\tfrac{1}{2}kw^2\kappa)^2 = -(\tfrac{1}{2}k\overline{w}^2\overline{\kappa} + \tfrac{1}{2}kw^2\kappa)^2 \leqslant 0. \tag{38}$$

Because $H = (\tfrac{1}{2}k\overline{w}^2\overline{\kappa})^2 + (\tfrac{1}{2}kw^2\kappa)^2 \geqslant 0$ and because the maximum of $G - H$ is zero, the maximum value of α is unity.

The upper bound on the alignment product, i.e., $\alpha = 1$, is simply a statement, parametrized for the case of Gaussian modes, of the fact that the second law of thermodynamics cannot be violated in phase space. If the bound could be exceeded, two or more independent low-powered modes could be combined into one higher-powered (higher-brightness) mode; e.g., one laser could be perfectly aligned while other independent lasers at the same frequency, which were offset or tilted from the aligned laser, could also feed with high coupling efficiency into the same fiber mode.

From Eq. (38), α is unity if and only if

$$\overline{w}^2\overline{\kappa} + w^2\kappa = 0. \tag{39}$$

Equation (39) identifies all alignment-plane combinations of $\overline{w}$, $\overline{\kappa}$, w, and κ that yield a maximum product ($\alpha = 1$). From Eq. (3) a simple mixed-representation form of Eq. (39) is

$$\overline{w}/\overline{w}_0 = w/w_0. \tag{40}$$

Equation (39) requires that $\overline{\kappa}$ and κ be of opposite sign; thus Eq. (40) is limited to those cases where the waists are on opposite sides of the alignment plane. In the waist-spacing representation Eq. (39) becomes

$$\overline{w}_0^2/\overline{z} + w_0^2/z = 0. \tag{41}$$

Equation (41) requires that the waists be on opposite sides of the alignment plane, each at a distance that is proportional to its waist area. (Think of each projection of an elliptical beam as if it were the projection of a circular beam.) Alternatively, for two waists of any size and spacing, Eq. (41) gives the position of the only alignment plane for which $\alpha = 1$. If α is maximized in the waist-spacing representation, Eq. (41) is the initial result, and Eqs. (39) and (40) then follow.

Equations (21) and (33) imply in conjunction with the bound on α that

$$\theta_e \leqslant 2^{-1/2}(1/\overline{w}_0^2 + 1/w_0^2)^{1/2}\lambda/\pi \tag{42}$$

with equality if and only if the rotation is about the point $\overline{z}$ or z given by Eq. (41). Note that the maximum value of θ_e depends on the waist sizes but not on their separation s.

From Eq. (9), a necessary condition for maximum transmissivity ($\tau_a = 1$) is

$$\bar{\kappa} = \kappa, \tag{43}$$

which implies, of course, that $\bar{\kappa}$ and κ be of the same sign. Thus, from Eqs. (39) and (43), it is apparent that the simultaneous maximization of α and τ_a, i.e., $\alpha = 1$ and $\tau_a = 1$, can occur only if

$$\bar{\kappa} = \kappa = 0, \tag{44}$$

i.e., both beam waists must fall on the alignment plane. [Putting the alignment plane in the far fields of the waists does not yield $\tau_a = 1$ and $\alpha = 1$ simultaneously because κ does not approach zero fast enough; i.e., $\kappa \to 0$ as $z \to 0$ in Eq. (1), but $\tau_a \to 0$ as $s \to \infty$ in Eq. (10).] If, however, some transmissivity is to be traded away to achieve greater tolerances, Eqs. (39)–(41) give the designer a choice of waist positions with $\alpha = 1$.

At the one extreme the maximum value of α is unity. At the other extreme the non-negative product α can be made arbitrarily small [$\alpha \to 0$ as $\kappa = \bar{\kappa} \to \infty$ in Eq. (35)]. Thus we interpret α as a measure of the efficiency of a coupling design from the standpoint of tolerance. The parameter α is quite distinct from the usual measure of coupling efficiency (i.e., τ_a or T_a).

Having bounded α, we write Eq. (33) as

$$A = \tau_a \theta_e d_e = \frac{1}{\pi} \lambda \alpha = \frac{1}{\pi} \frac{\lambda_0}{n} \alpha \leq \frac{1}{\pi} \frac{\lambda_0}{n}, \tag{45}$$

where n is the refractive index of the medium in the gap between the source and sink, and λ_0 is the wavelength in air. Because α is independent[15] of n [Eq. (35)], Eq. (45) shows that A scales as the wavelength λ. Introduction of a fluid ($n > 1$) into the gap reduces A and is thus inferior in this sense to the alternative of adding antireflection coatings to the source and sink. The fluid introduces additional phase shift between tilted wave fronts and nominally affects only θ_e [Eq. (17)]. However, the bound on α may force a design trade-off, and thus d_e and τ_a may have to be compromised to restore partially the reduced θ_e. The index could be assimilated into a normalized alignment product $\alpha' = \alpha/n$ since the bounds on α' are also $0 < \alpha' \leq 1$, but we prefer the form of a later figure (Fig. 3) if Eq. (45) is written as

$$0 < \tau_a \theta_e d_e / \lambda = \alpha/\pi \tag{46}$$

$$\leq 1/\pi, \tag{47}$$

with λ the wavelength in the medium of the gap. For round beams

$$0 < T_a^{1/2} \theta_e d_e / \lambda = \alpha/\pi \tag{48}$$

$$\leq 1/\pi. \tag{49}$$

In Eq. (45), n is not necessarily the index in the alignment plane; rather n is the index of the medium occupied by the beam as it crosses the gap between the two optical elements. For example, if one element were subject to a torsional vibration or rotational strain about a y axis within that element (e.g., inside the circuit or fiber in Fig. 2), this axis would define an alignment plane ($\bar{z}$) of interest. The real modes that exist between the elements in Fig. 2 are extended as virtual modes to this alignment plane, and it is the interelement index n, not the actual index profile within the optical element at the alignment plane, that governs this extension.

As noted in Sec. IV, more than one rotation axis may be of concern. Consider, therefore, a fixed design (= fixed values of $\bar{w}_0$, w_0, and s) and a varying rotation axis; i.e., a varying position z of the alignment plane. Once α has been evaluated on a given alignment plane, it is easily evaluated on any other alignment plane; that is, only θ_e in the product $\tau_a \theta_e d_e$ changes [Eq. (21)], and the new value of θ_e is found immediately from Eqs. (2) and (17). This dependence on z is also usefully approximated in the manner of Eq. (25); that is, fitting the Gaussian approximation

$$A(z)/A_{\max} = \alpha(z)/\alpha_{\max} = \theta_e(z)/\theta_{e,\max} = \exp[-(z - z')^2/(\delta z)^2] \tag{50}$$

to the exact result [Eqs. (2) and (17)] at $z = z'$ and using Eq. (21) yield

$$\delta z/\lambda = (-\tfrac{1}{2}\theta_e^{-1} d^2\theta_e/dz^2)_{z=z'}^{-1/2}$$

$$= 2^{1/2}\pi\tau_a (d_e/\lambda)^2 = 2^{1/2}(d_e/\lambda)/\theta_{e,\max} = 2^{1/2}/\pi\tau_a\theta_{e,\max}^2, \tag{51}$$

where z' is the value of z which satisfies Eq. (41), and $\theta_{e,\max} = \theta_e(z = z')$ is the value of θ_e given by Fig. 3 or by the equality form of Eq. (42), i.e., $\theta_{e,\max}$ is the value of θ_e at $\alpha = 1$. In a typical application one chooses a particular alignment plane and designs at $\alpha = 1$ for that plane. Then the design value of θ_e is $\theta_{e,\max}$, and δz, as given by Eq. (51), is an indication of how rapidly θ_e falls off with respect to rotation about axes at other values of z.

The conservation of the alignment product $\tau_a \theta_e d_e$ can also be interpreted from a classical-particle-beam phase-space viewpoint,[16] and, in fact, this particle limit motivated the present work. A sink (e.g., a detector or fiber) accepts a region of 2-D θ-d phase space equal to the θd product (etendue) of the original 2-D beam. The original beam is split reversibly into $1/\tau_a$ pencil beams, each with $1/\tau_a$ the etendue of the original beam. The one pencil beam that is retained then has τ_a times more phase space in which it can be misdirected without missing the fiber. In the classical-particle case, however, there is no finite wavelength to establish a lower bound on the phase space occupied by the beam. Alternately, a half-silvered mirror or a 3-dB coupler feeds two beams into one (doubles the initial etendue feeding a given final etendue) but does this at the expense of a 50% coupling efficiency. The functional form of the alignment product is apparent from these examples. This classical-particle model describes incoherent light and sound and has been applied, for example, to the coupling of light from a light-emitting diode into a multimode optical fiber.[17,18]

In the present section we have shown that any physically possible choice of τ_a, θ_e, and d_e satisfies Eq. (47). In the next section we show that any choice of the positive quantities τ_a, θ_e, and d_e satisfying

$$0 < \tau_a \leq 1, \tag{52a}$$

$$0 < \theta_e < \infty, \tag{52b}$$

$$0 < d_e < \infty, \tag{52c}$$

$$\alpha = \pi\tau_a\theta_e d_e/\lambda = 1, \tag{52d}$$

can be physically realized; i.e., one can always design at $\alpha = 1$ without introducing restrictions on the ranges of τ_a, θ_e, and d_e beyond those implied by $\alpha = 1$ and $\tau_a \leqslant 1$. It is this converse least-bound property that gives $A = \tau_a\theta_e d_e$ its usefulness and sets A apart from most other bounded functions of τ_a, θ_e, and d_e. (As a simple example, the product $P = \tau_a^2\theta_e d_e$ has the same bounds as A, but the upper bound of P cannot be achieved when $\tau_a < 1$.)

VII. Design Procedure

In many applications Eq. (52) implies that coupling efficiency should be deliberately traded away to achieve, for example, higher production yield from a self-aligning design or greater long-term stability of the coupling efficiency.[19] In such cases specific practical considerations would normally be introduced as a way of choosing among the many solutions, or approximate solutions, of Eq. (39), (40), or (41). However, the present work is limited to a demonstration by construction that every combination of the non-negative parameters τ_a, θ_e, and d_e that satisfies $\tau_a\theta_e d_e/\lambda = 1/\pi$ and $\tau_a \leqslant 1$ is physically realizable. As noted above [Eq. (44)], the case $\tau_a = 1$ implies planar wave fronts at the alignment plane, and so we will actually prove the stronger statement that every combination is possible within the class of beams that have their waists at the alignment plane ($\bar{z} = z = s = \bar{\kappa} = \kappa = 0$).

Because the waists are coplanar ($s = 0$), Eq. (29) applies; that is, the offset tolerance d_e and the axial tolerance s_e cannot be independently specified. For example, Eq. (52d) could just as well be written as

$$\alpha = 2^{-3/4}\pi^{1/2}\tau_a\theta_e(s_e/\lambda)^{1/2} = 1, \tag{53}$$

and various other forms are also possible if Eq. (51) is used. However, for this example we arbitrarily choose to design in terms of d_e rather than in terms of s_e or δz.

In decibel notation Eq. (52d) becomes

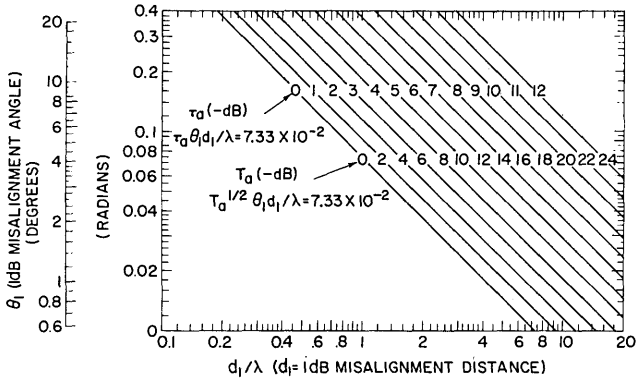

Fig. 3. Possible combinations of the circular-beam coupling efficiency T_a (or the elliptical-beam one-plane coupling efficiency τ_a), the 1-dB angular alignment tolerance θ_1, and the 1-dB offset tolerance d_1 when the alignment product $T_a^{1/2}\theta_1 d_1$ (or $\tau_a\theta_1 d_1$) is maximized.

$$\tau_a\theta_t d_s/\lambda = \frac{1}{\pi}\frac{\ln 10}{10}(st)^{1/2} \tag{54}$$

$$= 7.33\times10^{-2}(st)^{1/2} \tag{55}$$

$$= 7.33\times10^{-2}, s = t = 1, \tag{56}$$

where d_s is the offset where the loss is down by s dB, and θ_t is the angle where the loss is down by t dB; i.e.,

$$d_e = (10/s\ \ln 10)^{1/2}d_s = d_s/0.48s^{1/2}, \tag{57}$$

$$\theta_e = (10/t\ \ln 10)^{1/2}\theta_t = \theta_t/0.48t^{1/2}. \tag{58}$$

Equation (56) is plotted in Fig. 3. A design is begun with any point in Fig. 3 that is on or past the 0-dB line; i.e., with any choice of τ_a, θ_1, and d_1/λ that is consistent with Eqs. (52a) and (56). Corresponding to this design point we find below [Eq. (64) or (65)] two waist sizes $2w_+$ and $2w_-$. Because of the symmetry of the problem (i.e., either optical element can be regarded as the source because τ_a, θ_e, and d_e are bidirectional) there are two solutions; i.e., $\bar{w}_0 = w_+$, $w_0 = w_-$ and $\bar{w}_0 = w_-$, $w_0 = w_+$.

The ratio r of the waist sizes

$$r_+ = w_+/w_-, \qquad r_- = w_-/w_+ = 1/r_+ \tag{59}$$

is found by solving the $\bar{\kappa} = \kappa = 0$ case of Eq. (9) or the $s = 0$ case of Eq. (10) for r to yield

$$r_\pm = 1/\tau_a \pm (1/\tau_a^2 - 1)^{1/2}. \tag{60}$$

From Eqs. (9) and (21) the geometric mean waist size is given by

$$(\bar{w}_0 w_0)^{1/2} = (w_+w_-)^{1/2} = \tau_a^{1/2}d_e = 2.08\lambda\tau_a^{1/2}(d_1/\lambda). \tag{61}$$

Alternately, from Eqs. (9) and (17),

$$(\bar{w}_0 w_0)^{1/2} = (w_+w_-)^{1/2} = \lambda/\pi\tau_a^{1/2}\theta_e = 0.153\lambda/\tau_a^{1/2}\theta_1. \tag{62}$$

Because Eq. (44) satisfies Eq. (39) we already know that Eqs. (61) and (62) will yield the same value for $\bar{w}_0 w_0$. Nevertheless we verify this by equating the right-hand sides of Eqs. (61) and (62) and seeing that Eq. (52d) is indeed recovered. Finally the two mode widths are, from Eqs. (60) and (61),

$$w_\pm = r_\pm^{1/2}(w_+w_-)^{1/2} = r_\mp^{\pm1/2}(w_+w_-)^{1/2}. \tag{63}$$

$$= d_e[1 \pm (1 - \tau_a^2)^{1/2}]^{1/2}. \tag{64}$$

Alternately from Eqs. (60) and (62), or from Eqs. (64) and (52d),

$$w_\pm = [1 \pm (1 - \tau_a^2)^{1/2}]^{1/2}\lambda/\pi\tau_a\theta_e. \tag{65}$$

Because solutions always exist to Eqs. (60)–(65) over the physical parameter range, it follows that any point on or beyond the 0-dB line in Fig. 3 can be realized. (Of course, this small-angle Gaussian-beam model can be a poor representation of reality in extreme cases.) Figure 4 presents the results qualitatively, and Fig. 5 presents them quantitatively.

The curves in Fig. 5 have asymptotic values. Consideration of the limit $w_+ \to \infty$ yields from Eq. (42)

$$(10/\ln 10)^{1/2}\theta_1 = \theta_e \geqslant \frac{2^{-1/2}}{\pi}\frac{\lambda}{w_-}. \tag{66}$$

Consideration of the limit $w_- \to 0$ yields from Eq. (22)

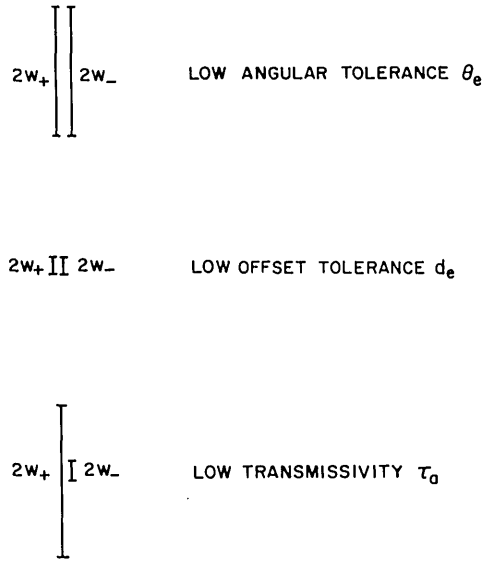

Fig. 4. Three cases where the source and sink waists ($2w_+$ and $2w_-$) of two round beams fall on the alignment plane. Each case takes a low value for one of the three parameters T_a, θ_e, and d_e to achieve high values for the other two. Case (a) has a low misalignment tilt tolerance θ_e. The large (compared to λ) waists mean that a large distance and hence a large phase shift open up between the waists with a small tilt angle. Case (b) clearly has a low offset tolerance d_e for vertical displacement of either waist. Case (c) has a low coupling efficiency T_a because of the disparity in waist size.

$$(10/\ln 10)^{1/2} d_1 = d_e \geq 2^{-1/2} w_+, \tag{67}$$

where in Eqs. (66) and (67) equality is the asymptotic value ($w_-/w_+ \to 0$). At $\tau_a = 1$ ($\tau_a = 0$ dB), the waists are equal ($w_+ = w_- = w_\pm$); then Eq. (17) yields

$$(10/\ln 10)^{1/2} \theta_1 = \theta_e = \frac{1}{\pi} \frac{\lambda}{w_\pm}, \tag{68}$$

and Eq. (21) yields

$$(10/\ln 10)^{1/2} d_1 = d_e = w_\pm. \tag{69}$$

The product of Eqs. (68) and (69) conforms to Eq. (36) as expected.

The design which results from Fig. 5, or from the preceding formulas in this section, may in a particular application be less easily fabricated than a design with more nearly equal waist sizes and with a separation s between the waists. In such a case a typical design procedure would be as follows: Starting with the same design values of τ_a, θ_e, and d_e, as permitted by Eq. (52), one chooses convenient waists sizes so that the design value of θ_e results from the equality form of Eq. (42). Because the waists are more nearly equal, Eq. (11) yields a value for τ_a at $s = 0$, which exceeds the design value of τ_a. Thus the waists are separated in either axial direction ($s > 0$ or $s < 0$) until Eq. (10) yields the design value of τ_a. The design value of d_e is then automatically acheived. Positioning of the waists with respect to the alignment plane in accord with Eq. (41) ensures that the separation does not change θ_e.

VIII. Laser–Fiber Coupling

As an example consider the design of a fiber tip for a $\lambda_0 = 1.3$ μm real-index-guided round-beam laser with

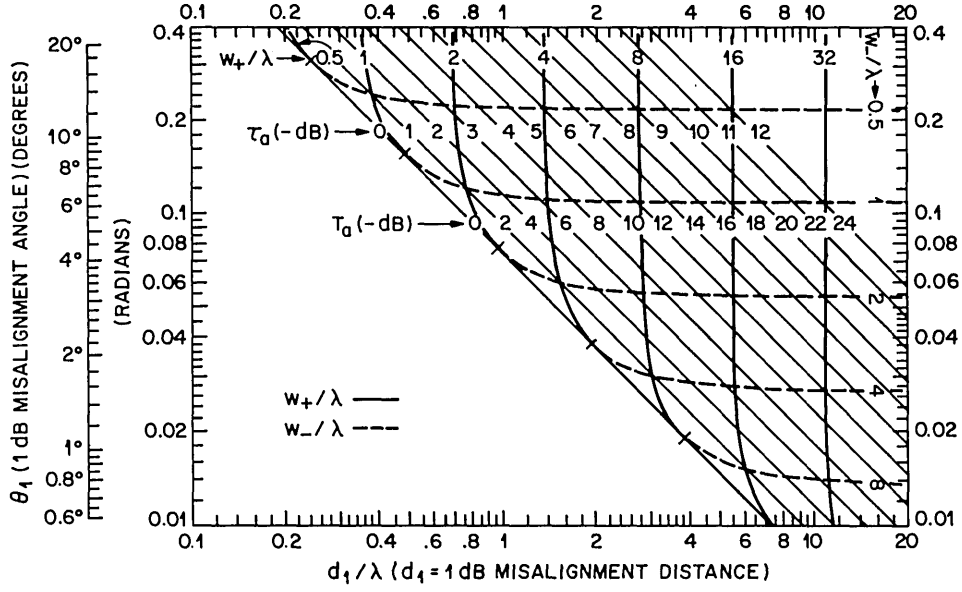

Fig. 5. That realization of Fig. 3 for which the beam waists, $2w_+$ and $2w_-$, fall on the alignment plane. The corresponding tolerance for axial separation of the waists is given by Eq. (29) or (30) using $d_e(0) = d_1/0.48$. The tilt tolerance for rotation about an axis outside of the plane of the waists is given approxmately by Eq. (51), where $\theta_{e,\max}$ is the value of θ_e from Fig. 5. To use Fig. 5 pick any two of five quantities and read off the other three. The five quantities are the two coplanar waists, $2w_+$ and $2w_-$, the 1-dB offset distance d_1, the 1-dB tilt angle θ_1, and the round-beam coupling efficiency T_a or the elliptical-beam one-plane coupling efficiency τ_a [Eq. (12)]. λ is the wavelength in the medium between the optical source and the sink.

a half-waist $\overline{w}_0 = 0.65\ \mu$m at the mirror face and an air gap (i.e., $\lambda = \lambda_0$) between the laser and fiber. We consider first that projection of parameter space which is spanned by Fig. 5. Figure 5 applies to the case where the fiber waist $2w_0$ and the alignment plane (the axis for θ rotation) are also on the laser face; that is, Fig. 5 considers the effect of varying the size of the fiber waist but not the effect of introducing an axial separation s between the waists.

If $w_0 < \overline{w}_0$, the laser half-waist $\overline{w}_0$ is w_+, the larger waist, and $\overline{w}_0/\lambda = w_+/\lambda = 0.65/1.3 = 0.5$. Thus as the fiber waist size $w_0 = w_-$ is varied by changing the taper or lens shape of the fiber, the varying design traces out the solid-line curve $w_+/\lambda = 0.5$ in the upper left corner of Fig. 5. If the fiber waist is larger than the laser waist, the laser waist becomes $2w_-$ ($\overline{w}_0/\lambda = w_-/\lambda = 0.5$), and the varying design traces out the dashed-line curve $w_-/\lambda = 0.5$ in Fig. 5. At $T_a = \tau_a^2 = 0$ dB, Fig. 5 or Eqs. (69) and (68), respectively, show that the offset tolerance has the objectionably small value $d_1 = (10/\ln 10)^{-1/2}\, 0.5\lambda = 0.31\ \mu$m, while θ_1 is an unnecessarily generous 17.5°. From Fig. 5, or from Eq. (64) solved for $\tau_a(w_-)$,

$$T_a = \tau_a^2 = 1 - [1 - (w_-/d_e)^2]^2, \qquad d_e \geq w_-, \tag{70}$$

it follows that doubling d_1 to 0.62 μm drops T_a by a, perhaps acceptable, 3.6 dB. [To find w_+ insert τ_a from Eq. (70) into Eq. (64) or use Fig. 5.] Correspondingly, Fig. 5, or Eq. (65), or Eq. (52d) shows that θ_1 is reduced to a still generous 13.2°. Thereafter, the $w_-/\lambda = 0.5$ curve begins to flatten out leaving θ_1 virtually unchanged [Eq. (66)] while severely reducing T_a; e.g., if d_1 is quadrupled to 1.25 μm, θ drops only slightly more (to 12.6°), while T_a is down by 9.2 dB, which would be unacceptable in many applications. The problem is that transmissivity T_a, rather than angular tolerance θ_1, is primarily traded for increased displacement tolerance d_1. That is, we are approaching the limit

$$(10/\ln 10)^{1/2} d_1 = d_e < 2^{1/2} w_-/T_a^{1/2} \tag{71}$$

implied by Eqs. (52d) and (66) or by Eq. (21) where $2w_-$ is the laser waist.

Next we leave the space of Fig. 5 and revert to the earlier formulas in search of a larger d_1. The first way to leave Fig. 5 is to move the alignment plane (rotation axis). This is not helpful because it lessens θ_1 [see Eq. (42)] without affecting d_1 or T_a [see Eqs. (10) and (21)]. The only other way to leave Fig. 5 is to introduce a separation s between the waist. From Eq. (10) the separation reduces T_a and, thus, from Eq. (21) d_e is indeed increased as desired. However, the conservation of $T_a^{1/2} d_e$ [Eq. (21)] with increasing s is worse than the conservation of $T_a^{1/2}\theta_1 d_1$ along the $w_-/\lambda = 0.5$ curve as the fiber waist is increased at $s = 0$ (because θ_1 does decrease somewhat). For example, it costs 3.6 dB to double d_1 by increasing the fiber waist size, whereas the conservation of $T_a^{1/2} d_1$ (when s is varied) shows that it costs 6.0 dB to double d_1 by separating equal-sized waists.[20] Thus, we return to the space of Fig. 5 for the design and conclude from the preceding paragraph that in limited-loss applications d_e will typically range from $\overline{w}_0$ ($T_a = 0$ dB) to $2\overline{w}_0$ ($T_a = -3.6$ dB); that is, $0.5\overline{w}_0 < d_1 < \overline{w}_0$. To get large d_1 with limited loss the laser waist $2\overline{w}_0$ must, therefore, be large. Large w_0 could be achieved by a phased array, or by resorting to a weakly confining active region, or by adding an optical transformer inside the laser (e.g., a taper of the confining region near the face of a distributed-feedback laser or an evanescently coupled passive layer) or external to the laser. If the external transformer is first fixed relative to the laser, perhaps lithographically, the present paper describes the final critical alignment of the source (laser plus transformer) with the sink (fiber with lensed tip or other transformer). If the laser subsequently creeps while the relative positions of the laser transformer, fiber, and fiber transformer remain fixed, this paper is again applicable with a source that consists of the laser and a sink that consists of the fiber and both transformers. If the laser transformer alone creeps, much of this work is again applicable after allowing for the fact that offset laser–transformer creep is equivalent to laser creep as scaled by the waist magnification ratio of the laser transformer etc.

After the first few decibels have been given away, the two methods (increasing the fiber waist size and separating the laser and fiber waists) become nearly equivalent (because of the slow change in θ_1 at greater decibels on a given dashed w_-/λ in Fig. 5), and it may be easier, if even more decibels are to be traded away for increased d_1, to start to separate the waists. Thus, since typical fiber modes are appreciably larger than typical laser modes, it follows that in many applications a lenseless fiber, with additional waist separation (= mechanical gap in this case) as required for adequate d_1, is rather close to the optimum (minimum reduction in T_a) way to get large d_1. (A taper or lens is necessary only if d_1 at the minimum practical gap is larger than required; i.e., only if the corresponding T_a is too small.) When a design uses both a size mismatch ($w_+ = w_0 > \overline{w}_0 = w_-$) and a waist separation s to achieve a given value of d_1, the unnecessary decrease in T_a can be found by comparing the actual $T_a = \tau_a^2$ from Eq. (10) with the theoretical maximum T_a from Eq. (70). In Eq. (70) $2w_- = 2w_0$ is the laser waist.

IX. Summary

Using a small-angle elliptic-Gaussian-beam model [Eqs. (15) and (16)] we have quantified the transmissivity-alignment trade-off for optical or acoustical couplers. Similar properties of the alignment product $A = \tau_a \theta_e d_e$ apply to classical-particle beams.

References

1. H. Kogelnik, "Coupling and Conversion Coefficients for Optical Modes in Quasi-Optics," Microwave Research Institute Symposia Series 14 (Polytechnic Press, New York, 1964), pp. 333–347. Our expressions for d_e and θ_e differ from Kogelnik's corresponding results.
2. D. Marcuse, *Light Trasnmission Optics* (Van Nostrand, New York, 1972), Chap. 6.
3. D. Marcuse, "Loss Analysis of Single-Mode Fiber Splices," Bell Syst. Tech. J. **56**, 703 (1977).

4. D. D. Cook and F. R. Nash, "Gain-Induced Guiding and Astigmatic Output Beam of GaAs Lasers," J. Appl. Phys. **46**, 1660 (April 1975).
5. H. Kuwahara, M. Sasaki, and N. Tokoyo, "Efficient Coupling from Semiconductor Lasers into Single-Mode Fibers with Tapered Hemispherical Ends," Appl. Opt. **19**, 2578 (1980).
6. G. D. Khoe, J. Poulissen, and H. M. de Vrieze, "Efficient Coupling of Laser Diodes to Tapered Monomode Fibers with High-Index End," Electron. Lett. **19**, 205 (1983).
7. G. Wenke and Y. Zhu, "Comparison of Efficiency and Feedback Characteristics of Techniques for Coupling Semiconductor Lasers to Single-Mode Fiber," Appl. Opt. **22**, 3837 (1983).
8. J. H. Rowen, unpublished.
9. R. E. Wagner and W. J. Tomlinson, "Coupling Efficiency of Optics in Single-Mode Fiber Components," Appl. Opt. **21**, 2671 (1982).
10. W. L. Emkey, "Optical Coupling between Single-Mode Semiconductor Lasers and Strip Waveguides," IEEE/OSA J. Lightwave Technol. **LT-1**, 436 (June 1983).
11. There may also be Fresnel-reflection loss at the sink which should be accounted for separately. Often the normal-incidence reflectivity is a sufficiently accurate estimate. Light reflected back into the source may, of course, change the source-output power, but that is a separate question from the coupling efficiency. The aligned losses arising from aberrations and other causes of non-Gaussian beams are found in some cases as by-products when the Gaussian fit is determined by projection.
12. All integrals in this paper are of the standard Gaussian form

$$\int_{-\infty}^{\infty} \exp(-ax^2 - 2bx - c)dx = (\pi/a)^{1/2} \exp(b^2/a - c),$$

where the real part of a is positive.
13. If one or both beams are astigmatic, the waist separation s_x in the x-z plane may differ from the waist separation s_y in the y-z plane; i.e., $s_y - s_x = \Delta s$. Nevertheless the forms of Eqs. (27), (28), and (30) are still valid, in the independent x-z and y-z planes approximation, if properly interpreted. From Eq. (12) it is apparent that, as the source-sink separation is varied, the maximum of T_a does not occur at the separations where $\tau_{a,x}$ and $\tau_{a,y}$ have their maxima. Equations (27) and (28) are still valid if s in Eq. (27) is replaced by S, the distance from the maximum point of T_a. From Eqs. (10) and (21) it follows that $d_{e,x}(0)$ in Eq. (30) is measured at the maximum of $\tau_{a,x}$, i.e., at that separation where $d_{e,x}$ is a minimum and similarly $d_{e,y}(0)$ is measured at that separation where $d_{e,y}$ is a minimum.
14. J. S. Cook, W. L. Mammel, and R. J. Grow, "Effect of Misalignment on Coupling Efficiency of Single-Mode Optical Fiber Butt Joints," Bell Syst. Tech. J. **52**, 1439 (1973).
15. $\overline{w}, w, \overline{\kappa}, \kappa$, and α are independent of n in the design sense that, for a given n, lenses and tapers are then chosen to yield the given values for the beam sizes and curvatures.
16. W. B. Joyce, "Classical Particle Description of Photons and Phonons," Phys. Rev. D **9**, 3234 (1974).
17. W. B. Joyce, R. Z. Bachrach, R. W. Dixon, and D. A. Sealer, "Geoemtrical Properties of Random Particles and the Extraction of Photons from Electroluminescent Diodes," J. Appl. Phys. **45**, 2229 (1974).
18. P. P. Deimel, "Integral Lens Design Considerations," to be published.
19. W. B. Joyce and B. C. DeLoach, "Alignment-Tolerant Optical-Fiber Tips for Laser Transmitters," unpublished.
20. Designing at $s = 0$ also has the advantage for nonastigmatic beams of facilitating the axial-direction alignment. That is, the design point ($s = 0$) corresponds to the easily recognized maximum in $\tau_a(s)$.

Of Optics *continued from page 4178*

preparation, high fluorine glass and chalcogenide glass research for mid-IR fiber transmission, polarization-maintaining fibers, and optical switch development.

NTT Ibaraki is noted for its significant contributions to the attainment of ultralow loss silica fibers, achieving losses of 0.2 dB/km at 1.55 μm in 1979. They have also been noted for their work on preparing single-mode fibers by the VAD process. Until recently, most single-mode fiber fabrication has been done by the modified chemical vapor deposition (MCVD) process. In fact, one of the major differences between U.S. and Japanese practices in fiber manufacture is the Japanese specialization in the VAD technique. The VAD process is the nearest thing to a quasi-continuous process, which is preferable to batch-type processing such as MCVD or OVPO (outside vapor phase oxidation). Only MCVD or OVD fibers are commercially available from U.S. vendors. The NTT work on VAD has been emulated by the major Japanese fiber suppliers such as Sumitomo, Furukawa, and Fujikura. Essentially, the VAD process involves the deposition of silica soot on the substrate by multiple flames to achieve a graded or step-index profile. The preform is subsequently sintered, collapsed, and elongated in separate steps before furnace drawing. The principal advantage over MCVD is the capability of producing very large preforms of high quality from which multikilometer lengths of fiber may be pulled. NTT has a small group devoted to the improvement of this process.

We next were shown the laboratory where research activity is very intense in mid-infrared fiber technology. Research in mid-infrared fiber technology is brisk in Japan and, in particular, at NTT. The group at NTT Ibaraki has heavily contributed to advances in the area. Although infrared fibers have been around for some time in the form of bundles for short distance imaging, the prospect for applying them to telecommunications is of recent realization since the discovery of glass forming heavy metal fluorides by Professor J. Lucas and his associates at the University of Rennes. The interesting feature of these materials is that theoretical loss spectra indicate extremely low transmission and scattering losses in the 2–6 μm range. Estimates are that losses of the order of 10^{-3} dB/km are attainable. If this goal is realized, the implications for long distance, unrepeatered data transmission are enormous. Other applications include new and innovative sensors, high power optical transmission, and wideband color multiplexing.

The NTT group is concentrating on the so-called halide glasses (BeF_2, ZrF_4, HfF_4, AlF_3/BaF_2, etc.) and chalcogenide glasses (As_2S_3, As_2Se_3, GeS_3, etc.). This group recently reported losses as low as 10 dB/km in the halide glasses at 2.5 μm. The major contributors have been Drs. Tadashi Miyashita, Toyotaka Manabe, and S. Mitachi along with their associates, T. Kanamori, K. Jinguji, Y. Ohishi, and M. Horiguchi. The preparation of halide fibers is done by two methods: in one technique, a core is cast in a mold and the cladding is poured around the core to make preforms. In the other method, the cladding glass is poured into a mold, the outer surface is allowed to cool below the glass transition temperature and the center part is poured out while still fluid. Subsequently, the central region is filled with core glass and the system is annealed to form the preform. Fibers are subsequently drawn in an electrical furnace. The Naval Research Laboratory uses a variation of this process, called the rotating casting technique, in which the cladding glass is spun in a cylindrical mold while cooling; then the central region is filled with core glass. There is a multitude of glass forming halides which can be used. The compositions may be binary, ternary, or quaternary or even simple fluorides of the zirconate family (ZrF_4, BaF_2, GdF_3, AlF_3). Although fibers have been successfully drawn and the NTT group can achieve losses as low as 10 dB/km at 2.5 μm, further progress has been plagued by scattering and impurity absorption from metal ions such as Fe^{3+}, etc. These ions are very difficult to remove by standard purification methods such as sublimation. The NTT group is attempting to re-

continued on page 4201